NSP NUCLEAR SYSTEMS PROGRAMS

# THERMAL DESIGN PROCEDURES FOR SPACE RANKINE CYCLE SYSTEM BOILERS

J. R. Peterson
Nuclear Systems Programs, Missile and Space Division,
General Electric Company, Evendale, Ohio, Building D, Mail Drop O-2
R. N. Weltmann
M. U. Gutstein
NASA–Lewis Research Center, Cleveland, Ohio, Mail Stop 500-201

Presented at
INTERSOCIETY ENERGY CONVERSION
ENGINEERING CONFERENCE
Boulder, Colorado
August 13–16, 1968



Nuclear Systems Programs
Space Systems
GENERAL ELECTRIC
Missile and Space Division
Cincinnati, Ohio 45215

# THERMAL DESIGN PROCEDURES FOR SPACE RANKINE CYCLE SYSTEM BOILERS

J. R. Peterson
Nuclear Systems Programs, Missile and Space Division,
General Electric Company, Evendale, Ohio, Building D, Mail Drop O-2
R. N. Weltmann
M. U. Gutstein
NASA-Lewis Research Center, Cleveland, Ohio, Mail Stop 500-201

## ABSTRACT

A boiler design procedure based upon correlations of experimental data is presented and employed to design a once-through counterflow potassium boiler for an advanced Rankine cycle space power system. The procedure considers nonuniform axial distribution of heat flux and four distinct heat transfer regions; namely, the superheat, transition, nucleate and subcooled regions. The effects of several variables upon boiler tube length are shown and optimization procedures discussed. The design procedure is shown to predict the length of a single tube once-through mercury boiler within about 15%.

## I. INTRODUCTION

Advanced potassium Rankine space power systems[1,2,3] use a once-through, liquid heated counterflow multiple tube boiler to vaporize the working fluid which drives a turboalternator. Since dry vapor is required for the turbine, the working fluid is superheated before it leaves the boiler tubes. The working fluid entering the boiler is substantially subcooled and has to be preheated to a temperature above the saturation temperature before boiling and vaporizing can commence. In the boiling region of a counterflow boiler, the heat flux continuously increases up to a maximum at the point of critical heat flux. Downstream of the point of critical heat flux the generally continuous annular liquid film which occurs for wetting fluids is believed to become disrupted and the heat transfer coefficient decreases to the superheated vapor value at 100% quality. Through the superheat region the heat transfer coefficient remains essentially constant. Because of the above described heat transfer trends, it becomes important to delay the point of critical heat flux so that it occurs at a high quality. Helical inserts which swirl the flow have been shown[4] to delay the onset of the critical heat flux condition at the expense of increased working fluid pressure drop. As this pressure drop increases for constant boiler exit conditions, the heating to working fluid temperature difference at boiling inception (the pinch-point) decreases, making liquid superheat and slug flow instabilities more likely. Consequently a procedure is required for optimized boiler design which recognizes the complex problems described above.

In this paper, correlations derived from recent forced convection boiling potassium experiments[4,5] are summarized, and a design procedure for once-through liquid heated potassium counterflow boilers is presented. This procedure is an attempt to improve prediction accuracies by recognizing the principal local aspects of once-through potassium boiling demonstrated by test data while still retaining sufficient simplicity for usefulness in practical design. The design of an example boiler obtained by the procedure which has operating conditions typical of an advanced potassium space power system is also presented. The influence on this boiler design of insert twist ratio is indicated. The effects of heating fluid inlet temperature and flow rate as well as changes in vapor exit variables, such as saturation and superheat temperatures are also shown. An indication of the general validity of

[1] J. P. Davis and G. M. Kikin, "Lithium-boiling potassium Rankine cycle test loop operating experience," Presented to Second Intersociety Energy Conversion Engineering Conference, August 13–17, 1967.

[2] R. E. English and R. N. Weltmann, "Experience in investigation of components of alkali-metal-vapor space power systems," Proceedings of Symposium on Alkali Metal Coolants – Corrosion and System Operating Experience sponsored by the International Atomic Energy Agency, Vienna, Austria, November 28–December 2, 1966, Published 1967.

[3] M. A. Zipkin, "Components and systems design for a 400 kw Rankine cycle space power system," Presented to Second Intersociety Energy Conversion Engineering Conference, August 13–17, 1967.

[4] J. R. Peterson, "High performance 'once-through' boiling of potassium in single tubes at saturation temperatures of 1500°F to 1700°F," NASA CR-842, August, 1967.

[5] J. A. Bond and G. L. Converse, "Vaporization of high- temperature potassium in forced convection at saturation temperatures of 1800°F to 2100°F," NASA CR-843, July, 1967.

the design procedure for wetting fluids is presented by comparison of predicted and experimental data from a single tube mercury boiler operated under wetting conditions.

## II. DESIGN CORRELATIONS

The heat transfer and pressure loss equations employed for the thermal design procedure presented in this paper are summarized following. These equations are essentially empirical correlations of recent test data obtained near the operating conditions of space Rankine cycle potassium boilers. The forms of the equations employed, however, are derived from considerations of the flow regimes and heat transfer mechanisms indicated by the data to occur at the conditions of interest. The predictions of the effects of the helical inserts upon heat transfer and pressure loss are based in addition upon information obtained from single phase air and water insert evaluation experiments. The design correlations are derived and discussed in more detail elsewhere.[4,5] Figure 1 shows the typical axial heat flux and heat transfer coefficient distribution through a counter-flow boiler tube. The configuration of the single vane helical inserts employed in the boiler tubes for many of the tests is shown in Figure 2.

Figure 1 illustrates the four distinct heat transfer regions suggested by the test data and assumed by the design procedure to occur in a once-through potassium boiler. The subcooled liquid region is defined as the region from the potassium inlet to the point of boiling initiation. Similarly the point of boiling initiation marks the beginning of the nucleate boiling region, which extends until the local vapor quality and heat flux become high enough such that only partial wetting of the tube wall occurs. The region of partial wetting is defined as the transition boiling region and the point separating this region from the nucleate boiling region is defined as the critical heat flux point. The fourth heat transfer region is the superheated vapor region, which extends from the point of 100% quality to the potassium boiler exit. If the tube wall-to-potassium temperature difference is high enough to cause a dry-wall condition (the Leidenfrost state), there will also be a film boiling region extending over the entire boiler tube or a portion of it. Film boiling was not observed in the liquid metal heated potassium boiler tests discussed in Reference 4.

The heat transfer and pressure loss relations established for the four distinct heat transfer regions are summarized following. Care must be exercised in extrapolating these relations beyond the range of test data, especially in the two-phase regions, since heat transfer mechanisms and flow regimes different than those appropriate to the experimental data may be encountered. Listings of the range of test variables and discussions of the flow regimes and heat transfer mechanisms upon which the correlations are based are presented along with the design equations. The correlations are presented proceeding from the potassium vapor exit to the potassium liquid inlet, since the design calculations are performed in this order.

### Superheated Vapor Region

The heat transfer coefficient and frictional pressure loss for a tube containing a helical insert are predicted in terms of the values calculated for the same tube without insert at the same vapor mass velocity.

$$h_{gH} = (h_{gA}) \left[ \left( \frac{L_H}{L} \right)^{0.8} \left( \frac{D_i}{D_e} \right)^{0.2} \right] \quad (1)$$

$$\Delta P_{gH} = (\Delta P_{gA}) \left[ \left( \frac{L_H}{L} \right)^{2.75} \left( \frac{D_i}{D_e} \right)^{1.25} \right] + \Delta P_{gM} \quad (2)$$

The vortex effect is accounted for by the multiplier term shown in brackets. The bare tube pressure loss ($\Delta P_{gA}$) is calculated from the Blasius equation[6] and the bare tube heat transfer coefficient ($h_{gA}$) is calculated from the Dittus Boelter equation.[6] The momentum pressure loss ($\Delta P_{gM}$) is calculated as follows:

$$\Delta P_{gM} = \frac{G^2 \overline{\left( \frac{L_H}{L} \right)^2}}{g_c} \Delta (1/\rho_g) \quad (3)$$

The helical parameters in equations (1) through (3) were derived assuming solid body rotation[4] and are as follows:

$$\frac{L_H}{L} = \frac{V_H}{V} = \sqrt{1 + \left( \frac{\pi D_i}{p} \right)^2} \quad (4)$$

$$\frac{D_e}{D_i} = \frac{1 - \left( \frac{D_{cb}}{D_i} \right)^2}{1 + \frac{D_{cb}}{D_i} + \frac{1}{\pi} \left( 1 - \frac{D_{cb}}{D_i} \right)} \quad (5)$$

[6] W. H. McAdams, "Heat Transmission," McGraw-Hill, New York, 1954.

where

$$\left(\frac{L_H}{L}\right)^2 = \frac{1}{3}\left[\left(\frac{L_H}{L}\right)^2 + \left(\frac{L_H}{L}\right)\left(\frac{L_H}{L_{cb}}\right) + \left(\frac{L_H}{L_{cb}}\right)^2\right] \quad (6)$$

$$\frac{L_H}{L_{cb}} = \sqrt{1 + \left(\frac{\pi D_{cb}}{p}\right)^2} \quad (7)$$

Figure 3 shows a comparison of equations (1) and (2) with experimental helical flow heat transfer coefficients and frictional pressure loss data obtained with air for a Reynolds Number of 75,000. The range of conditions encompassed by the data are as follows:

| | |
|---|---|
| Insert Twist Ratio | 0.5 to 6.0 |
| Superficial Reynolds Number | 30,000 to 300,000 |
| Tube-To-Fluid Temperature Difference | 60° F to 110° F |

The secondary flow caused by insert radial acceleration is not considered in the relations presented. The reason is that this mechanism is expected to become significant at large insert twist ratios. As can be seen from Figure 3, good agreement with the prediction is obtained up to the largest twist ratio tested.

Another mechanism for heat transfer occurring in the superheated vapor region not considered by equation (1) is heat transfer by thermal radiation. Direct radiation to the potassium vapor is negligible, but radiation from the tube wall to the insert structure with subsequent secondary forced convection to the vapor can be significant. This radiation to the insert structure amounts to 10-15% of the total heat transferred for the example design presented subsequently and is calculated using procedures presented by Bond.[5]

## Transition Boiling Region

Equation (8) is a correlation of transition boiling heat transfer data which were obtained in several single tube liquid metal heated potassium test boilers.[4] The form of the equation reflects the heat transfer mechanism thought applicable in the transition boiling region. This mechanism can be boiling or evaporation of patches or rivulets of liquid in conjunction with forced convection heat transfer from dry areas. The constants and exponents appearing in equation (8) are empirically determined from experimental potassium data.

$$h_{TB} = h_{gH}\left[1 + \frac{2.55 \times 10^{+5}\left(\frac{1-x}{x}\right)^{0.7}\left(1+a_R\right)^{1/5}}{\Delta t_w^{\,2}}\right] \quad (8)$$

The vapor phase forced convection heat transfer coefficient ($h_{gH}$) appearing in equation (8) is computed from equation (1) and $\Delta t_w$ is the tube wall to potassium temperature difference, averaged over the increment employed. The radial acceleration developed by the insert is calculated as follows:

$$a_R = \frac{2}{g_o D_i}\left[\frac{x\,G}{\rho_g\sqrt{\frac{\rho_f}{\rho_g}}}\,\frac{\pi D_i}{p}\right]^2 \quad (9)$$

Equation (8) and the experimental potassium transition boiling data are shown in Figure 4. The experimental data cover the following ranges of test variables:

| | |
|---|---|
| Insert Twist Ratio | 2, 6 and No Insert |
| Insert Acceleration | 0 to 140 g's |
| Wall-to-Potassium Temperature Difference | 58° to 244° F |
| Vapor Quality | 44% to 93% |
| Saturation Temperature | 1512° to 1704° F |
| Tube Internal Diameter | 0.67 to 0.92-inches |

## Nucleate Boiling Region

Potassium, due to its relatively small vapor to liquid density ratios at temperatures of interest, has a large void fraction for flow in pipes at low quality. At a quality of 5%, for example, the void fraction calculated[5] for a temperature range of 1500° F to 2100° F varies from 75% to 50%, respectively, increasing with increase in quality. Furthermore, at the high fluxes characteristic of the potassium once-through boiler, the boiler tube length associated with the low quality region is short. Only about 2% of the total tube length is typically required to increase the vapor quality from zero to 5%. It is expected, therefore, that the bubble and slug flow regimes characteristic of low void fractions will be very short or absent in high performance once-through boiling. The flow regime thought to be characteristic of the nucleate boiling region is the annular-mist regime which consists of a thin continuous liquid film wetting the boiler tube wall with some of the liquid entrained in the vapor core. Two vaporization mechanisms are possible for potassium under these conditions. At the high heat fluxes encountered in the nucleate boiling region of a once-through potassium boiler (typically in excess of 200,000 Btu/hr-ft$^2$), sufficient wall superheat is attained for bubble nucleation. At low heat fluxes, on the other hand, heat can be conducted through the thin liquid film with subsequent evaporation from the vapor-liquid interface without bubble nucleation

at the tube wall. Converse[5] gives quantitative predictions regarding the onset of nucleation for the annular mist flow regime. The correlating equation employed for the nucleate boiling region reflects the bubble nucleation mechanism thought to occur, being based upon a superposition of nucleate pool boiling and liquid forced convection as recommended by Kutateladze.[7] Figure 5 shows the correlation employed. The experimental nucleate boiling heat transfer coefficients are divided by the corresponding heat transfer coefficients predicted by the superposition procedure and the ratio plotted against the insert acceleration, yielding an empirical correlation of the insert effects as follows:

$$h_{NB} = \sqrt{h_{PB}^2 + h_f^2}\left[0.7 - (1 + a_R) \times 10^{-3}\right] \quad (10)$$

The nucleate pool boiling heat transfer coefficient ($h_{PB}$) is that predicted by Bonilla[8] and the liquid forced convection coefficient ($h_f$), calculated for the total flow rate, is that predicted by Rohsenow.[9] The ranges of test variables appropriate to the data defining the correlation for the nucleate boiling heat transfer coefficient are as follows:

| | |
|---|---|
| Tube Diameter | 0.42 to 0.92-inches |
| Heat Flux | 50,000 to 250,000 Btu/(hr-ft$^2$) |
| Saturation Temp. | 1500° F to 2100° F |
| Insert Acceleration | 100 to 440 g's |
| Insert Twist Ratio | 2 to 6 |

Equation (10) is recommended over the range of insert acceleration from 100 to 440 g's. Additional test data obtained in a constant heat flux test section[5] are available for bare tubes and for tubes with inserts at low acceleration values. These data scatter considerably, but are generally higher than predicted by equation (10), as suggested by the dotted line on Figure 5. The constant heat flux data are local measurements whereas the other data of Figure 5 were obtained from liquid metal heated test sections and are averaged over an increment of the tube length. The local data scatter more than the incremental data. The reason could be that a local temperature measurement can be substantially affected by perturbations in liquid film thickness and momentary dry spots with controlled heat flux conditions.

## Film Boiling

There are currently insufficient potassium film boiling data available in the literature upon which to base a correlation. Film boiling is not predicted to occur at the conditions typical of liquid heated space Rankine cycle potassium boilers. However, film boiling can occur at extreme operating conditions. In this case, it is recommended that equation (1) be employed to compute the heat transfer coefficient at the local vapor velocity. This procedure is indicated to be conservative by comparison with exploratory potassium film boiling data reported by Bond.[5]

## Two-Phase Pressure Loss

The two-phase multiplier technique of Martinelli-Nelson[10] extended to potassium by Converse[5] is employed for calculation of potassium frictional pressure loss in all two-phase regions. The calculation is illustrated by equation (11) where $\Phi$ is the integrated Martinelli multiplier and $\Delta P_f$ is the corresponding pressure loss computed for the liquid at the total flow rate. The liquid pressure drop is calculated using equation (2) with liquid properties.

$$\Delta P_{FTP} = \Delta P_f \, \Phi \quad (11)$$

The integrated Martinelli multiplier for a particular quality increment under consideration is obtained by numerical integration of the local Martinelli multipliers presented graphically by Converse.[5]

There is a momentum pressure loss in addition to the frictional loss in two-phase regions due to quality and vapor density changes. The momentum pressure loss used is given by equation (12).

$$\Delta P_{MTP} = \frac{G^2 \left(\frac{\bar{L}_H}{L}\right)^2}{g_c} \Delta \frac{1}{\hat{\rho}} \quad (12)$$

where as shown by Converse,[11]

$$\frac{1}{\hat{\rho}} = \frac{1}{\rho_g}\left[(1 - x)\frac{\rho_g}{\rho_f} + x\sqrt{\rho_g/\rho_f}\right]\left[1 + x\left(\sqrt{\rho_f/\rho_g} - 1\right)\right] \quad (13)$$

[7] S. S. Kutateladze, "Fundamentals of Heat Transfer," Academic Press Inc., New York, 1963.

[8] C. F. Bonilla, M. M. Weiner, and H. Bilfinger, "Pool boiling of potassium," Oak Ridge National Laboratory, September 5, 1963.

[9] W. M. Rohsenow, "Developments of Heat Transfer," M.I.T. Press, Cambridge, 1964.

[10] R. C. Martinelli and D. B. Nelson, "Prediction of pressure drop during forced-circulation boiling of water," TRANS. ASME, vol. 70, p. 695, 1948.

[11] J. Longo, "Alkali metal boiling and condensing investigations," Quarterly Progress Report No. 6, Contract NAS 3-2528, General Electric Company, April 20, 1964, NASA CR 54037.

Representative experimental boiling potassium pressure loss data obtained at 1700° F are compared with the Martinelli prediction for the same temperature in Figure 6. Also shown on the same figure is a prediction obtained assuming homogeneous flow (slip = 1). Generally, better agreement with the experimental data is obtained with the Martinelli prediction which, in addition, yields higher and therefore more conservative values than does the homogeneous flow prediction. The ranges of test variables over which potassium pressure loss data have been obtained are as follows:

| | |
|---|---|
| Tube Diameter | 0.67 to 0.92-inch |
| Insert Twist Ratio | 2 to 6 |
| Saturation Temperature | 1500° F to 2100° F |
| Vapor Quality | 0 to 100% |
| Mass Velocity | 15 to 150 lb/ft$^2$-sec |

## Liquid Heat Transfer

The single phase heat transfer coefficients for the primary heating fluid and subcooled potassium liquid required for boiler design are obtained from predictions published in the literature. The correlation of Lubarsky and Kaufman[12] applicable to flow in tubes is employed for the potassium heat transfer coefficient in the subcooled heating region as follows:

$$\frac{h_f D_e}{k_f} = 0.625 \, (N_{Pe})^{0.4} \qquad (14)$$

Equation (14) is used since it was found applicable by Bond[5] for liquid potassium heat transfer data for a tube containing a vortex generating insert. The liquid potassium pressure loss is generally small and is ignored.

The predictions recommended by Dwyer[13] and Maresca and Dwyer[14] are employed to calculate the primary fluid heat transfer coefficient. The equation used for an annulus (single tube boiler) is:

$$\frac{h_p D_e}{k_p} = \alpha + \beta (E \, N_{PeP})^{\gamma} \qquad (15)$$

where

$\alpha = 4.63 + 0.686Y$

$\beta = 0.02154 - 0.000043Y$

$\gamma = 0.752 + 0.01657Y - 0.000883Y^2$

[12] B. Lubarsky and S. J. Kaufman, "Review of experimental investigations of liquid-metal heat transfer," NASA Report No. 1270, 1956.

[13] O. E. Dwyer, "Eddy-transport in liquid metal heat transfer," AiChE J., 9, pp. 261–8, 1963.

[14] M. W. Maresca and O. E. Dwyer, "Heat transfer to mercury flowing in-through a rod bundle," J. Heat Transfer 86, pp. 180, 1964.

The constant Y in this case is defined as the ratio of shell inside diameter to tube outside diameter. For a tube bundle, the prediction is as follows:

$$\frac{h_p D_{es}}{k_p} = 6.66 + 3.12Y + 1.184Y^2 + 0.0155 \, (E \, N_{PeP})^{0.86} \qquad (16)$$

The constant Y for a tube bundle is defined as the spacing between tube centers divided by the tube outside diameter. The parameter E for both equations is presented graphically by Rohsenow[9] and Dwyer[13] and is the ratio of the eddy diffusivity for heat to the eddy diffusivity for momentum.

## Heat Transfer Criteria

Criteria determining the lengths of the various heat transfer regions in the boiler tube are required for design in addition to heat transfer and pressure loss correlations for the regions themselves. Film boiling can occur anywhere in the boiler if the local tube wall-to-potassium temperature difference is above the value necessary to establish the Leidenfrost condition or spheroidal state. The temperature difference for onset of film boiling with inserts is indicated by the exploratory forced convection film boiling data reported by Bond[5] to be approximately 300° F. The data reported by Poppendiek[15] for individual potassium droplets also suggest the value to be about 300° F. This value of 300° F is therefore used to determine the onset of film boiling.

The equations appropriate to the superheated vapor region are employed from the potassium exit to the point in the boiler tube where the vapor quality is 100%. The transition boiling region extends from the point of 100% quality, or the initiation of film boiling if it is present to the point of critical heat flux. The critical heat flux point in a counterflow boiler is defined as the point of maximum two phase heat flux in the boiler tube (Figure 1).

The critical heat flux condition is predicted to occur when the local heat flux and vapor quality satisfy the following equation:

$$q_c'' = \frac{(1 + a_R)^{1/4} \times 10^6}{1 + 2\left(\frac{x_c}{1 - x_c}\right)} \qquad (17)$$

[15] H. F. Poppendiek, et al., "Quarterly technical report on high acceleration field heat transfer for auxiliary space nuclear power systems," AEC Contract No. AT(04-3)-409, September 1 through November 30, 1964, Geoscience Ltd., Solana Beach, California.

Equation (17) is an empirical correlation of potassium critical heat flux data obtained over the following ranges of test conditions.

| | |
|---|---|
| Tube Diameter | 0.42 to 0.92-inches |
| Saturation Temp. | 1522° to 2100° F |
| Critical Heat Flux | 50,000 to 400,000 Btu/(hr-ft$^2$) |
| Critical Quality | 40% to 95% |
| Mass Velocity | 16 to 101 lb/(ft$^2$-sec) |
| Insert Twist Ratio | 2 to 6 and No Insert |
| Insert Acceleration | 0 to 195 g's |

Equation (17) is shown with the experimental critical heat flux data in Figure 7.

The nucleate boiling region extends from the point of critical heat flux to the point of boiling inception. Boiling is assumed to be initiated at zero quality for design purposes. Depending upon the specified operating conditions, however, the bulk liquid may be either subcooled or superheated with respect to its local saturation temperature at boiling initiation. The degree of superheat or subcooling can be predicted if the dimensions of the largest active (vapor or gas-filled) nucleation site are known. The bulk liquid superheat at boiling inception ($\Delta t_{LS}$) is given in terms of the nucleation cavity radius $r_c$, and the primary fluid to potassium temperature difference at boiling inception ($\Delta t_{OIB}$) as follows.

$$\Delta t_{LS} = \frac{2\sigma}{r_c}\frac{Tv_{fg}}{Jh_{fg}} - \frac{\Delta t_{OIB}}{1 + \frac{h_f}{h_{Pw}}} \qquad (18)$$

The first term in equation (18) is the wall superheat required to nucleate a bubble of radius $r_c$[9] and the second term is the calculated wall-to-bulk temperature difference for the liquid. To be effective, a nucleation cavity must hold entrapped vapor or inert gas, whose presence or absence is determined in a complex manner by operating history and conditions, purity levels and cavity configurations. Equation (18) therefore is most useful in predicting qualitative trends.

## III. THERMAL DESIGN PROCEDURE

The potassium boiler thermal design procedure outlined herein is formulated to yield the heat transfer area and thus the boiler tube length required to meet a specified boiler operating point. The procedure has been set up to permit optimization for minimum weight, pressure drop, etc., depending upon the selection of different boiler configurations and insert twist ratios. In order to accomplish this, it is necessary that the calculations proceed from the working fluid boiler exit to the boiler inlet, treating the boiler tube length and working fluid pressure loss as dependent or output variables. The length and pressure loss for each of the heat transfer regions from the superheated region to the boiling and subcooled regions are determined in sequence, the total length and pressure loss of the boiler tube being the sum of the values for each of the four regions. By this approach, a unique solution is obtained for specified boiler exit conditions. The variables which define a boiler operating or design point are tabulated as follows:

Table 1

BOILER INPUT VARIABLES

Thermal Power
Heating Fluid Inlet Temperature
Heating Fluid Temperature Change or Flow Rate
Working Fluid Inlet Temperature
Working Fluid Exit Saturation Temperature
Working Fluid Exit Quality or Superheat
Boiler Tube Material
Boiler Tube Diameter and Wall Thickness
Number of Tubes and Tube Spacing
Insert Twist Ratio (p/D)

The boiler tube material and wall thickness are determined by stress and metallurgical considerations. The boiler tube diameter, number of tubes, and tube spacing are selected by consideration of boiler weight, fabricability and reliability as well as system requirements such as primary fluid pressure loss and boiler configuration. The insert geometry and twist ratio can be optimized for minimum weight, minimum pressure loss, etc., by performing the thermal design calculations for several insert geometries and twist ratios.

The thermal design calculational procedure involves the simultaneous iterative solutions of interdependent heat transfer, energy and pressure loss equations. The calculations are performed over successive increments of tube length proceeding from the specified conditions at the working fluid boiler exit until the specified working fluid boiler inlet temperature is obtained.

As the calculations proceed through the boiler tube, the heat transfer and pressure loss equations are changed for each of the heat transfer regions. The length of each region is determined by the correlations and criteria previously presented. The following table presents the output results that can

be obtained from the design procedures.

Table 2

THERMAL DESIGN PROCEDURE OUTPUT RESULTS

Heating Fluid
- Heat Transfer Coefficient
- Axial Temperature Distribution

Working Fluid
- Length of Each Region
- Heat Transfer Coefficient for Each Region
- Heat Transferred in Each Region
- Pressure Loss in Each Region
- Axial Temperature Distribution
- Average Heat Flux
- Total Pressure Loss
- Total Tube Length

The design scheme described makes no attempt to evaluate boiler stability, since this depends on the system as well as on the boiler. The results of Berenson[16] with multiple tube boilers suggest that system stability is improved by the use of flow resistances at the liquid inlets of the boiler tubes. It is known, in addition, that boilers having bulk liquid superheat at boiling inception and appreciable tube lengths in the low quality slug flow regime are potentially unstable. These conditions are generally encountered at low saturation temperatures and low heat fluxes and should be examined in any boiler design.

## IV. EFFECTS OF MAJOR DESIGN VARIABLES

A computer program based on the previously described thermal design procedure has been written. As illustration of the use of this program, an example boiler sized in accordance with the thermal design procedure is presented. In addition, the effects on the geometry of this boiler of different insert twist ratios, working fluid exit superheats and exit saturation temperatures and heating fluid inlet temperatures and flowrates are discussed to indicate the parametric information which can be obtained from the design procedure.

### Example Boiler

For the computation of the example boiler, a heated, countercurrent flow configuration was selected. The boiler was assumed to transfer 3.3 MW of heat and to have 55 3/4-inch OD tubes in a 9.3-inch diameter shell. Each tube contains a helical insert with a twist ratio (p/D) of 2.0. This twist ratio was selected to result in minimum heat transfer area. A sketch of this boiler is shown in Figure 8. Table 3 presents the input specifications which are the input data for the design procedure. The output data for the example boiler are also shown in Table 3.

Table 3 shows that for the design specifications employed, the example potassium boiler has a total length of 89-inches, which is made up of a 7-inch subcooled liquid region, a 26-inch nucleate boiling region, a 13-inch transition boiling region and a 43-inch superheat region. The average heat flux for this boiler is 158,000 Btu/hr-ft$^2$. The thermal design procedure indicates that a lithium heated counterflow potassium boiler of relatively compact physical dimensions can transfer 3.3 MW (thermal) of heat. The lithium and potassium temperatures are shown in Figure 9 as a function of boiler length. The overall temperature difference at boiling inception (the "pinch-point") is approximately 50° F for this design as can be seen from the figure. The magnitude of the pinch-point is important since the tendency for bulk liquid superheat at boiling inception and the tendency for slug flow become greater as the pinch-point becomes smaller. If the boiler tubes for the example design have a nucleation cavity size distribution similar to that observed by Converse and Bond[5] for boiling potassium in a Cb–1Zr tube (0.05 to 0.2 mils radius) equation (18) predicts that boiling will be initiated with the bulk liquid subcooled for the example design.

### Effect of Insert Twist Ratio Variation

The example boiler was sized using a helical insert twist ratio of 2.0. Figure 10 illustrates the effect upon boiler length of varying this ratio, assuming all other specifications given in Table 3 are held constant. Figure 10 is a plot of the ratio of boiler tube length to the tube length of the example boiler as a function of helical insert twist ratio. Figure 11 shows the effect of insert twist ratio upon the predicted potassium pressure drop occurring after boiling inception normalized to that of the example boiler of Table 3. The pressure drop of the subcooled liquid potassium region is small, of the order of 0.1 psi, and is not included in Figure 11.

As the insert twist ratio is reduced (Figure 10) the boiler tube length initially becomes shorter since the insert acceleration increases potassium heat transfer performance. At an insert twist ratio of 1.75,

[16] P. J. Berenson, "An experimental investigation of flow stability in multiple tube forced-convection vaporizers," ASME Paper 65-HT-61, Presented at the ASME AIChE Heat Transfer Conference, Los Angeles, California, August 8–11, 1965.

Table 3

INPUT SPECIFICATIONS AND OUTPUT RESULTS
3.3 MW EXAMPLE BOILER DESIGN

Input Specifications

| | |
|---|---|
| Thermal Power | 3.3 MW |
| Material of Construction | T-111 Alloy |
| Number of Tubes | 55 |
| Tube Spacing (Center-to-Center) | 1.125-inch |
| Tube Outside Diameter | 0.75-inch |
| Tube Wall Thickness | 0.040-inch |
| Helical Insert p/D (1/4-inch Centerbody) | 2.0 |
| Lithium Inlet Temperature | 2200° F |
| Lithium Outlet Temperature | 2100° F |
| Potassium Inlet Temperature | 1100° F |
| Potassium Outlet Temperature | 2150° F |
| Potassium Outlet Saturation Temperature | 2050° F |

Output Results

| | |
|---|---|
| Total Tube Length | 89-inches |
| Shell Inside Diameter | 9.3-inches |
| Average Heat Flux | 158,000 Btu/(hr-ft$^2$) |
| Lithium Flow Rate | 29 lb/sec |
| Lithium Heat Transfer Coefficient | 9100 Btu/(hr-ft$^2$-°F) |
| Approximate Lithium Pressure Loss | 2 psi |
| Potassium Pressure Loss | 9 psi |
| Length of Subcooled Heating Region | 7-inches |
| Subcooled Liquid Heat Transfer Coefficient | 1500 Btu/(hr-ft$^2$-°F) |
| Length of Nucleate Boiling Region | 26-inches |
| Nucleate Boiling Heat Transfer Coefficient | 17,000 Btu/(hr-ft$^2$-°F) |
| Length of Transition Boiling Region | 13-inches |
| Transition Boiling Heat Transfer Coefficient | 2600 Btu/(hr-ft$^2$-°F) |
| Length of Superheated Vapor Region | 43-inches |
| Superheated Vapor Heat Transfer Coefficient | 102 Btu/(hr-ft$^2$-°F) |

the boiler tube length is a minimum and further reductions of the twist ratio increase the estimated tube length. This increase of tube length at small twist ratios is due to increasing potassium temperature levels in the boiler, since the exit pressure is held constant. Consequently, the lithium-to-potassium temperature difference in the boiling region decreases and longer boiler tubes are required to compensate for this effect.

Figures 10 and 11 indicate that the designer may select a particular boiler length from a wide range of lengths by an appropriate choice of insert twist ratio. However, as the figure shows, the potassium pressure drop increases as the tube length decreases. This result suggests that requirements placed by system considerations on boiler size and pressure drop will influence the selection of the insert twist ratio. The twist ratio of 2.0 used for the example design was selected instead of 1.75 to yield near minimum tube length with some margin for error.

## Effect of Boiler Exit Superheat and Exit Saturation Temperature

Figure 12 is a plot of the ratio of predicted boiler tube length to the tube length of the example boiler as a function of potassium exit superheat with potassium exit saturation temperature as a parameter. This plot was obtained with the thermal design procedure and the specifications of Table 3, with the exception that the potassium exit conditions were varied. The helical twist ratio was identical to that shown in Table 3.

Figure 12 indicates that substantial increases in tube length are required to achieve moderate increases in potassium exit superheat because the superheated vapor heat transfer coefficient is small, on the order of 100 Btu/hr-ft$^2$-°F. Increasing the required exit saturation temperature likewise requires longer tube lengths because of the reduction of the average lithium-to-potassium temperature difference.

## Effect of Lithium Inlet Temperature and Flow Rate

Figure 13 is a plot of boiler tube length, normalized to the tube length for the example design, as a function of lithium flow rate with lithium inlet temperature as parameter. The lithium temperature change through the boiler is directly related to the lithium flow rate and is shown in addition to lithium flow rate as the abscissa scale of Figure 13. All parameters other than those varied are the same as listed in Table 3.

Figure 13 shows that substantial increases in tube length are required as the lithium temperature change increases for a particular value of

lithium inlet temperature. Higher values of lithium temperature change (lower lithium flow rates) are possible with no increase in boiler size if the lithium inlet temperature is also increased. These effects are due to changes in average lithium-to-potassium temperature difference. This average temperature difference decreases with decreases in either lithium flow rate or lithium inlet temperature, requiring corresponding increases in heat transfer area.

### Effect of Potassium Inlet Temperature

The subcooled heating length, as shown in Figure 9 and Table 3, is less than 10% of the total boiler length. Potassium inlet temperature therefore has a minor effect upon tube length and boiler size. However, low potassium inlet temperatures cause large lithium to potassium temperature differences, creating large temperature gradients in the tube walls and header and producing mechanical design problems due to thermal stress. The thermal stresses in the boiler tubes and in the potassium inlet tube header must be examined and appropriate thermal baffles incorporated when these stresses become large.

## V. APPLICATION OF THE DESIGN PROCEDURES TO A SINGLE TUBE MERCURY BOILER

The preceding correlations were derived from heat transfer and pressure loss data obtained with potassium test boilers, and a procedure using these correlations was applied to the design of an example space potassium boiler. A single tube potassium boiler, representative of one tube from the example design is being prepared for test. In addition, a single tube counterflow NaK heated mercury boiler with vortex generator insert, designed using the same procedure with modified correlations, has been tested. This boiler was fabricated with a tantalum tube which was wetted by mercury for the operating conditions employed.

The form of the correlations presented are thought to be general for wetting fluids other than potassium with suitable property changes if the heat transfer mechanisms used for potassium are applicable. For design of the mercury boiler, the following steps were taken. The superheat equations were assumed valid for mercury with appropriate physical properties. Film boiling was assumed not present. In the absence of applicable mercury transition boiling data, rivulet flow on the wall was assumed permitting an estimate of the transition heat transfer coefficient. The correctness of this estimated coefficient is difficult to assess since the length of the transition region is calculated to be only 10% of the length of the boiler and thus has a small influence on its overall thermal performance. The form of the potassium critical heat flux correlation was assumed for mercury. In the absence of applicable forced convection critical heat flux data for wetting mercury, a predicted pool boiling critical heat flux value[17,18] was used at zero quality and acceleration and a curve was drawn following the trend of equation (17). In the nucleate boiling region, the same superposition procedure as used for potassium was employed but insert effects were ignored since the acceleration values for mercury were low (about 20 g's). The liquid phase heat transfer correlations are general and were applied to the mercury boiler. The pressure drop predictions are also general and were used with appropriate property changes.

A comparison of the calculated and experimentally obtained data is given for the mercury boiler in the following table. Double containment was employed for the mercury. A 321 stainless steel outer boiler tube was positioned concentrically over the inner tantalum tube with static NaK in the annulus between the two. The tantalum tube outer diameter and wall thickness were 0.75-inch and 0.040-inch respectively while the stainless steel tube outer diameter and wall thickness were 0.875-inch and 0.035-inch. The double tube arrangement was positioned concentrically within a 321 stainless steel shell having an internal diameter of 1.38-inches. The NaK heating fluid flowed in the annulus between shell and inner stainless steel tube countercurrent to the mercury.

The specified NaK to mercury temperature difference at the mercury boiler exit was obtained in a boiler tube length of about 14.5 feet rather than the calculated 16.5-foot length indicating less than 15% error in predicting the boiler length.

## VI. CONCLUDING REMARKS

A procedure for designing liquid metal heated counterflow once-through boilers typical of advanced Rankine cycle space power systems has been presented. This design procedure is based on calculating in sequence the pressure drop and length of four distinct heat transfer regions. Results obtained by

[17] N. Zuber, "Stability of boiling heat transfer," TRANS. ASME, April 1958.

[18] S. S. Kutateladze, et al., "Liquid-Metal Heat Transfer Media," (Supplement of the Soviet Journal of Atomic Energy), Consultants Bureau, Inc., New York, 1959.

Table 4

COMPARISON OF PREDICTED AND EXPERIMENTAL RESULTS FOR A SINGLE-TUBE MERCURY BOILER

| | Experiment | Prediction |
|---|---|---|
| NaK Inlet Temperature | 1300° F | 1305° F |
| NaK Outlet Temperature | 1135° F | 1138° F |
| NaK Flow Rate | 1.95 lb/sec | 1.94 lb/sec |
| Thermal Power | 71.8 KW | 72.0 KW |
| Mercury Inlet Temperature | 350° F | 550° F |
| Mercury Exit Temperature | 1282° F | 1275° F |
| Mercury Exit Saturation Temperature | 1069° F | 1063° F |
| Specified NaK to Mercury Temperature Difference at Mercury Exit | 18° F | 30° F |
| Mercury Pressure Drop | 90 psi | 81 psi |
| Pinch-Point Temperature Difference | 38° F | 45° F |
| Mercury Flow Rate | 0.47 lb/sec | 0.47 lb/sec |
| Insert Twist Ratio | 1.94 | 2.0 |
| Tube Length | 16.0 ft | 16.5 ft |

application of this procedure to parametric studies indicate that the boiler tube length is shortened by using inserts which impart helical acceleration to the working fluid. This performance increase is paid for in terms of increased working fluid pressure drop. Large pressure losses were shown to cause small values of the lithium-to-potassium temperature difference at boiling inception (the pinch-point). As the pinch-point approaches zero, boiler lengths were shown to increase. Also, small pinch-points increase the likelihood of liquid superheat and slug flow instability. A proper design procedure must weigh the problem of small pinch-points against the performance gains obtained by increasing helical accelerations. Parametric data obtained by applying the design procedure suggest that the boiler tube length increases with increasing saturation temperature and increasing amounts of superheat, and that a constant power boiler increases in length with decreasing heating fluid flow rate and decreasing heating fluid inlet temperature.

An example boiler, typical in operating conditions for potassium Rankine space power systems, was designed using the procedure described in this paper. The insert configuration employed for the example potassium boiler was selected to provide near minimum heat transfer area with a potassium pressure loss of about 5% of saturation pressure and a pinch-point of about 50° F. An indication of the general applicability of the design procedure presented was obtained by an experimental test of a single tube once-through mercury boiler operated under wetting conditions which showed that the specified vapor exit conditions were obtained in a tube length within 15% of the predicted value. The procedure permits parametric design studies of once-through, liquid metal-heated counterflow boilers for a variety of operating conditions and geometries.

NOMENCLATURE

| Symbol | Definition | Units |
|---|---|---|
| $a_R$ | Radial Acceleration Produced by the Insert Divided by the Standard Acceleration of Gravity, number of g's | Dimensionless |
| $D_{cb}$ | Diameter of Insert Centerbody | ft |
| $D_e$ | Equivalent Tube Diameter for Helical Flow | ft |
| $D_{es}$ | Equivalent Diameter of Shell | ft |
| $D_i$ | Inside Diameter of Boiler Tube | ft |

## NOMENCLATURE

| Symbol | Definition | Units |
|---|---|---|
| $E$ | Ratio of the Eddy Diffusivity for Heat to the Eddy Diffusivity for Momentum | Dimensionless |
| $G$ | Mass Velocity | $lb_m/(ft^2\text{-}hr)$ |
| $g_c$ | Conversion Factor | $4.17 \times 10^8 (lb_m/lb_f) ft/hr^2$ |
| $g_o$ | Standard Acceleration of Gravity | $4.17 \times 10^8$ ft/hr$^2$ |
| $h_f$ | Heat Transfer Coefficient for Potassium Liquid | Btu/hr-ft$^2$-°F |
| $h_{fg}$ | Heat of Vaporization for Potassium | Btu/$lb_m$ |
| $h_{gA}$ | Gas Heat Transfer Coefficient Evaluated for Axial Flow | Btu/hr-ft$^2$-°F |
| $h_{gH}$ | Gas Heat Transfer Coefficient for Helical Flow | Btu/hr-ft$^2$-°F |
| $h_{NB}$ | Nucleate Boiling Heat Transfer Coefficient | Btu/hr-ft$^2$-°F |
| $h_P$ | Primary Fluid Heat Transfer Coefficient | Btu/hr-ft$^2$-°F |
| $h_{PB}$ | Pool Boiling Heat Transfer Coefficient | Btu/hr-ft$^2$-°F |
| $h_{Pw}$ | Combined Heat Transfer Coefficient of the Primary Fluid and the Tube Wall | Btu/hr-ft$^2$-°F |
| $h_{TB}$ | Transition Boiling Heat Transfer Coefficient | Btu/hr-ft$^2$-°F |
| $J$ | Mechanical Equivalent of Heat | 778 $lb_f$-ft/Btu |
| $k_f$ | Thermal Conductivity of Potassium Liquid | Btu/hr-ft-°F |
| $k_P$ | Thermal Conductivity of the Primary or Heating Fluid | Btu/hr-ft-°F |
| $\frac{L}{L_o}$ | Boiler Tube Length Divided by Boiler Tube Length Calculated for Example Boiler Design | Dimensionless |
| $\frac{L_H}{L}$ | Ratio of Helical Length to Axial Length, Evaluated at the Tube Wall | Dimensionless |
| $\left(\frac{L_H}{L}\right)^2$ | Mean Square Ratio of Helical Length to Axial Length | Dimensionless |
| $\left(\frac{L_H}{L_{cb}}\right)$ | Ratio of Helical Length to Axial Length, Evaluated at the Insert Centerbody | Dimensionless |
| $N_{Pe}$ | Peclet Number | Dimensionless |
| $N_{PeP}$ | Peclet Number of the Primary or Heating Fluid | Dimensionless |
| $p$ | Insert Pitch | ft |
| $p/D$ | Insert Twist Ratio, Axial Distance for 360° Revolution of Helix Vane | Dimensionless |
| $\frac{\Delta P}{\Delta P_o}$ | Potassium Pressure Loss Divided by Potassium Pressure Loss Calculated for Example Boiler Design | Dimensionless |
| $\Delta P_f$ | Liquid Pressure Drop | $lb_f/(ft^2)$ |
| $\Delta P_{FTP}$ | Friction Two-Phase Pressure Drop | $lb_f/(ft^2)$ |
| $\Delta P_{gA}$ | Gas Pressure Drop for Axial Flow | $lb_f/(ft^2)$ |
| $\Delta P_{gH}$ | Gas Pressure Drop for Helical Flow | $lb_f/(ft^2)$ |
| $\Delta P_{gM}$ | Momentum Pressure Drop for the Gas | $lb_f/(ft^2)$ |

## NOMENCLATURE

| Symbol | Definition | Units |
|---|---|---|
| $\Delta P_{MTP}$ | Momentum Two-Phase Pressure Drop | $lb_f/(ft^2)$ |
| $q''_c$ | Critical Heat Flux | $Btu/hr\text{-}ft^2$ |
| $r_c$ | Nucleation Cavity Radius | ft |
| $\Delta t_{LS}$ | Bulk Liquid Superheat at Boiling Inception | °F |
| $\Delta t_{OIB}$ | Overall Primary Fluid to Potassium Temperature Difference at Boiling Inception | °F |
| $\Delta t_w$ | Tube Wall-to-Potassium Temperature Difference | °F |
| T | Absolute Temperature | °R |
| $v_{fg}$ | Volume Change Upon Vaporization | $ft^3/lb_m$ |
| $\frac{V_H}{V}$ | Ratio of Helical to Axial Velocity at the Tube Wall | Dimensionless |
| x | Vapor Quality | Dimensionless |
| $x_c$ | Vapor Quality at the Point of Critical Heat Flux | Dimensionless |
| **Greek Symbols** | | |
| $\alpha, \beta, \gamma$ | Constants Defined in Text | |
| $\hat{\rho}$ | Mean Density for Two-Phase Flow, Defined in Text (Equation 13) | $lb_m/ft^3$ |
| $\rho_f$ | Liquid Density | $lb_m/ft^3$ |
| $\rho_g$ | Vapor Density | $lb_m/ft^3$ |
| $\Phi$ | Two-Phase Frictional Pressure Drop Multiplier, Ratio of Two-Phase Pressure Drop to that Calculated for the Liquid Flowing Alone | Dimensionless |
| $\sigma$ | Surface Tension | $lb_f/ft$ |

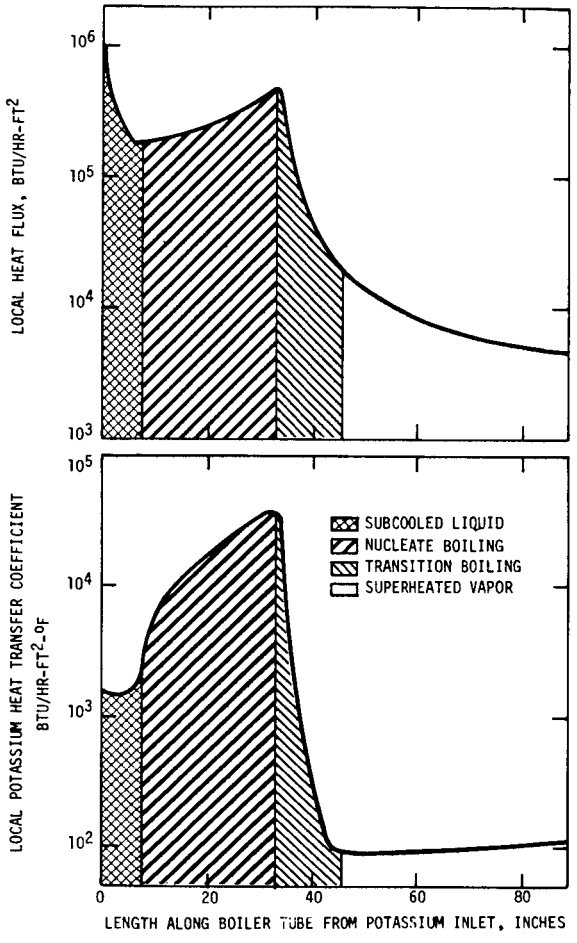


Fig. 1 – Typical Distribution of Heat Flux and Heat Transfer Coefficient in a Liquid-Heated, Counterflow Boiler Tube

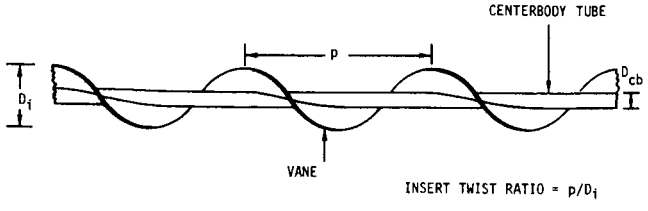


Fig. 2 – Configuration of Single Vane Helical Insert

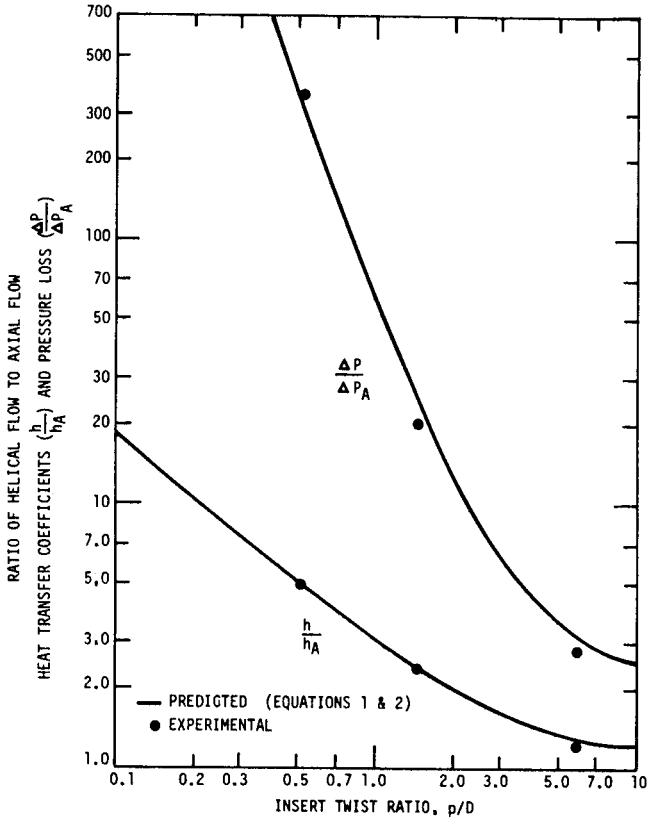


Fig. 3 – Single Phase Pressure Drop and Heat Transfer for Helical Inserts as a Function of Insert Twist Ratio

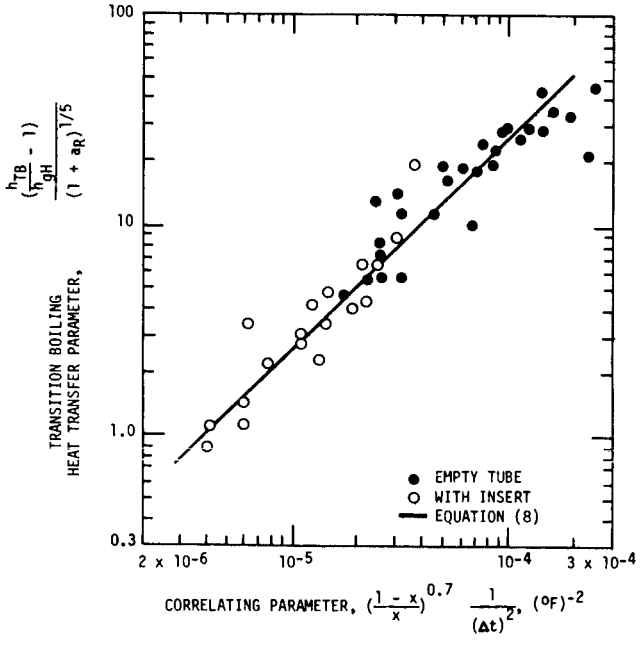


Fig. 4 – Potassium Transition Boiling Data and Correlation

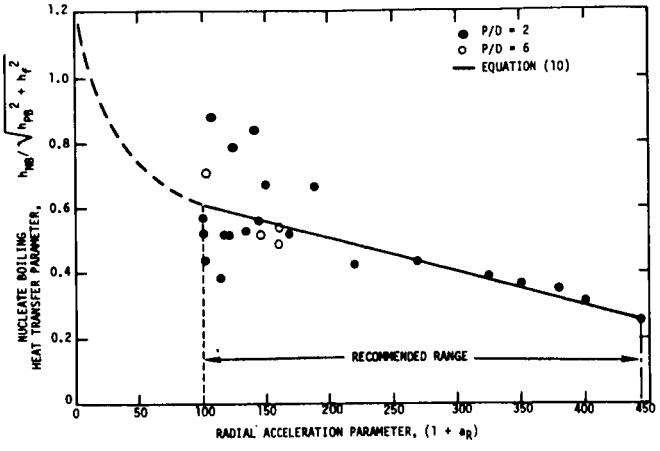


Fig. 5 – Potassium Nucleate Boiling Data and Correlation

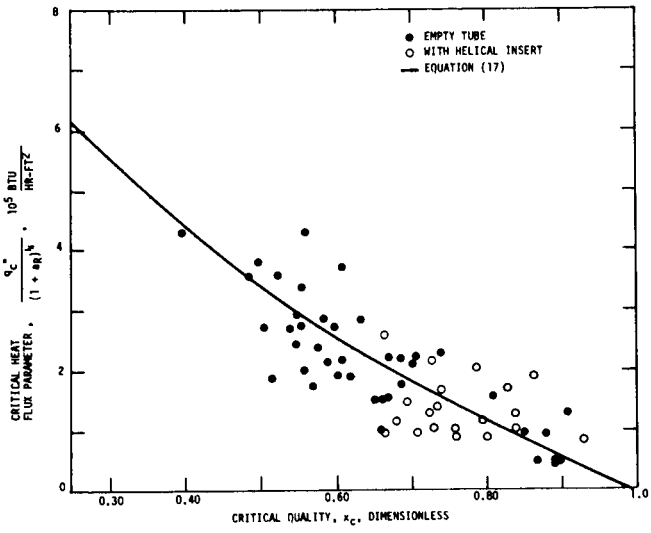


Fig. 7 – Potassium Critical Heat Flux Data and Correlation

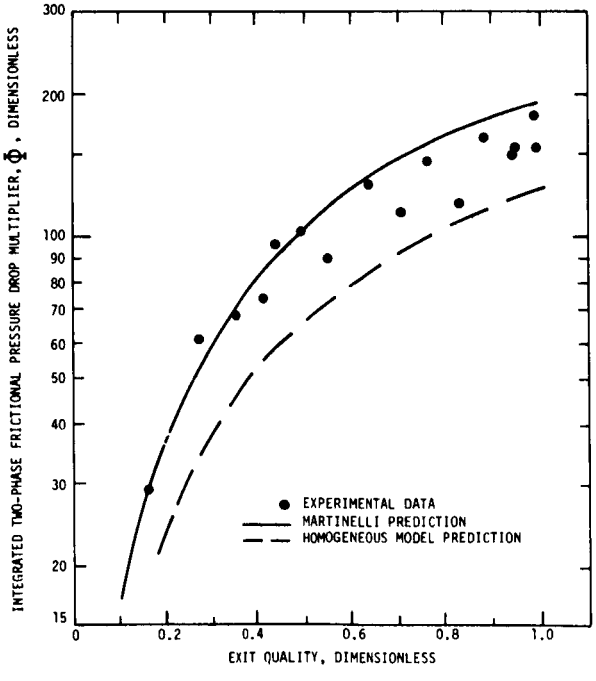


Fig. 6 – Potassium Boiling Pressure Loss Data and Correlation at 1700° F

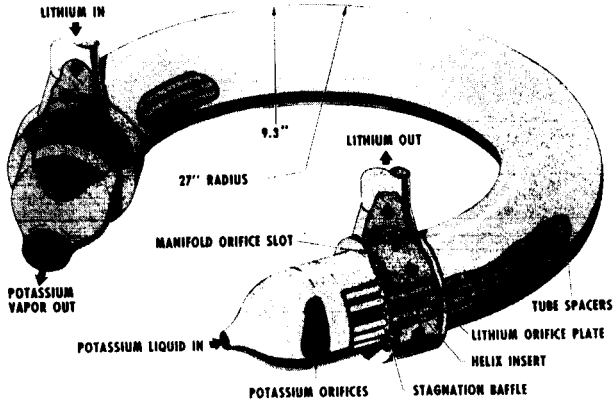


Fig. 8 – Conceptual Design of 3.3 $MW_t$ Once-Through Potassium Boiler

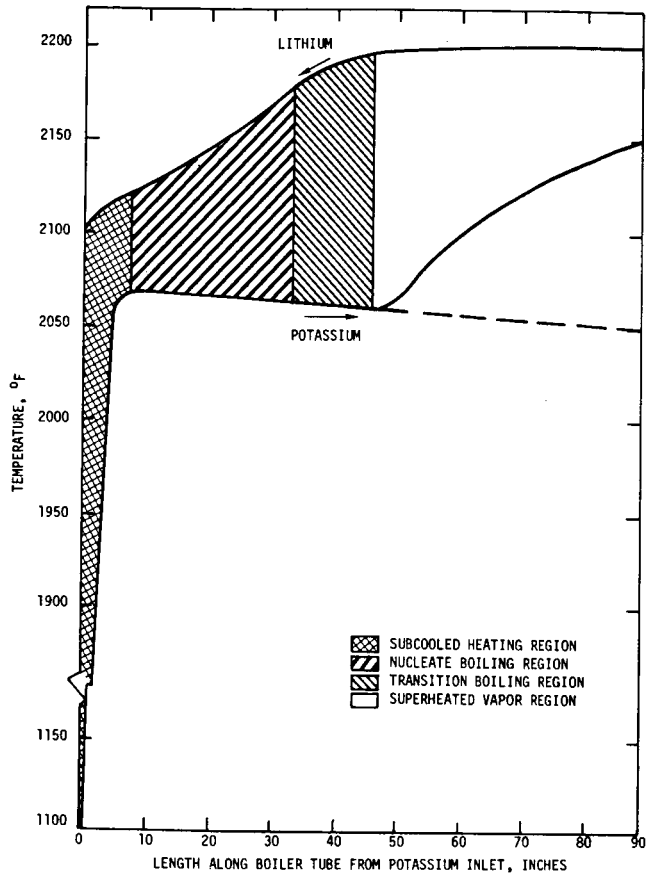


Fig. 9 – Axial Temperature Distribution for Lithium and Potassium in the Example Boiler

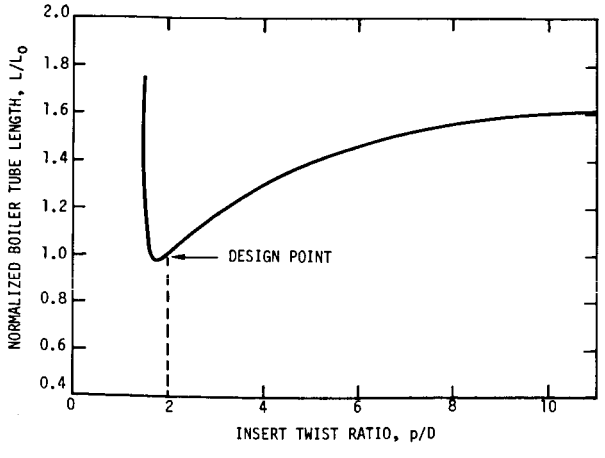


Fig. 10 – Effect of Insert Twist Ratio Upon Boiler Tube Length for the Example Design

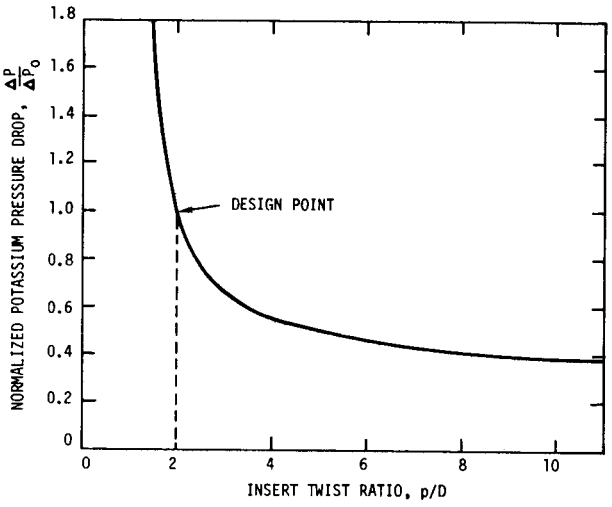


Fig. 11 – Effect of Insert Twist Ratio Upon Potassium Pressure Loss for the Example Design

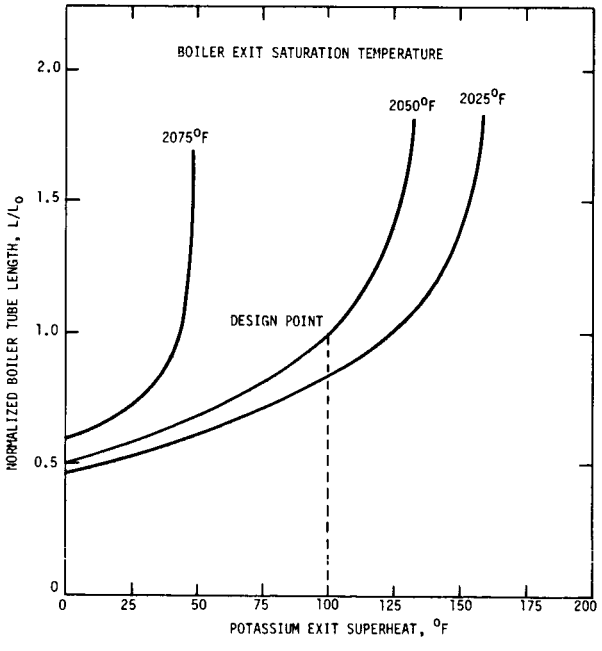


Fig. 12 – Effect of Boiler Exit Vapor Superheat and Boiler Exit Saturation Temperature Upon the Tube Length for the Example Design

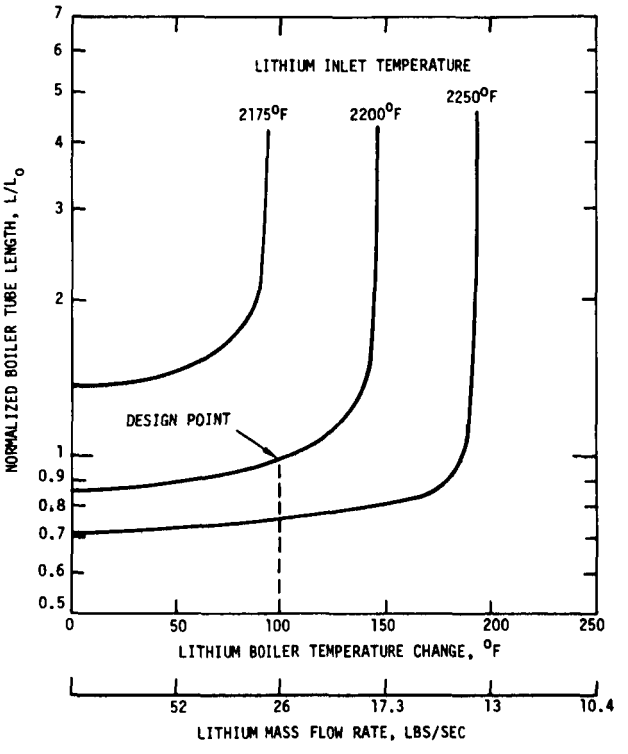


Fig. 13 – Effect of Lithium Boiler Temperature Change and Lithium Inlet Temperature Upon the Tube Length for the Example Design

ACKNOWLEDGMENT

This paper is based upon work performed under National Aeronautics and Space Administration Contracts NAS 3-2528 and NAS 3-9426.